

# TOP PRECISION FOR ASSOCIATED TOP-PAIR PRODUCTION PROCESSES AT THE LHC\*

ANNA KULESZA<sup>a</sup>, LESZEK MOTYKA<sup>b</sup>, DANIEL SCHWARTLÄNDER<sup>a</sup>  
TOMASZ STEBEL<sup>b</sup>, VINCENT THEEUWES<sup>c</sup>

<sup>a</sup>Institute of Theoretical Physics, WWU Münster, 48149 Münster, Germany  
<sup>b</sup>Institute of Theoretical Physics, Jagiellonian University, 30-348 Kraków, Poland  
<sup>c</sup>Institute for Theoretical Physics, Georg-August-University Göttingen  
 37077 Göttingen, Germany

*(Received May 22, 2020)*

The studies of the associated production processes of a top-quark pair with a colour-singlet boson, *e.g.* Higgs,  $W$  or  $Z$ , are among the highest priorities of the LHC programme. Correspondingly, improvements in precision of theoretical predictions for these processes are of central importance. In this paper, we review our latest results on resummation of soft gluon corrections. The resummation is carried out using the direct QCD Mellin space technique in three-particle invariant mass kinematics. We discuss the impact of the soft-gluon corrections on predictions for total cross sections and differential distributions.

DOI:10.5506/APhysPolB.51.1425

## 1. Introduction

The measurements [1–10] of associated production of a heavy boson ( $H, W, Z$ ) with a top–antitop quark pair provide an important test for the Standard Model at the Large Hadron Collider (LHC). These are the key processes to experimentally determine the top-quark couplings. In particular, the associated  $t\bar{t}H$  production directly probes the top Yukawa coupling without making any assumptions on its nature. Moreover, they are relevant in searches for New Physics due to both being directly sensitive to it and providing an important background. The  $t\bar{t}W$ ,  $t\bar{t}Z$  processes also play an important role as a background for the associated Higgs boson production process  $pp \rightarrow t\bar{t}H$ . Thus, it is necessary to know the theoretical predictions for  $pp \rightarrow t\bar{t}B$ ,  $B = H, W^\pm, Z$  with high accuracy, especially in the light of

---

\* Presented at XXVI Cracow Epiphany Conference on LHC Physics: Standard Model and Beyond, Kraków, Poland, January 7–10, 2020.

ever improving precision of cross-section measurements. For example, the very recent measurement of the  $t\bar{t}Z$  cross section [10] carries statistical and systematic errors of only 5–7%.

Fixed order cross sections up to next-to-leading order in  $\alpha_s$  have been for some time already known both for the associated Higgs boson [11, 12], and  $W$ - and  $Z$ -boson production [13, 14]. They were recalculated and matched to parton showers in [15–23]. Furthermore, QCD-EW NLO corrections are also known [24–26]. For the  $t\bar{t}H$  and  $t\bar{t}Z$  processes, the NLO QCD [27, 28] and EW corrections [29] to production with off-shell top quarks were also calculated. While NNLO calculations for this particular type of  $2 \rightarrow 3$  processes are currently out of reach, a class of corrections beyond NLO from the emission of soft and/or collinear gluons can be taken into account with the help of resummation methods. Such methods allow to account for effects of soft gluon emission to all orders in perturbation theory. Two common approaches to perform soft gluon resummation are either calculations directly in QCD or in an effective field theory, in this case soft-collinear effective theory (SCET).

For the associated  $t\bar{t}H$  production, the first calculations of the resummed cross section at the next-to-leading logarithmic (NLL) accuracy, matched to the NLO result were presented in [30]. The calculation relied on application of the traditional Mellin-space resummation formalism in the absolute threshold limit, *i.e.* in the limit of the partonic energy  $\sqrt{\hat{s}}$  approaching the production threshold  $M = 2m_t + m_H$ . Subsequently, resummation of NLL corrections arising in the limit of  $\sqrt{\hat{s}}$  approaching the invariant mass threshold  $Q$ , with  $Q^2 = (p_t + p_{\bar{t}} + p_H)^2$ , was performed in [31] and later extended to the next-to-next-to-leading-logarithmic (NNLL) accuracy and applied to the  $t\bar{t}H$  production [32], as well as  $t\bar{t}Z$  and  $t\bar{t}W$  production [33]. Apart from the total cross sections, also the distribution in the invariant mass  $Q$  [32–34], the transverse momentum of the boson  $B$ ,  $p_T(B)$ , [34, 35], the invariant mass  $m_{t\bar{t}}$  of the  $t\bar{t}$  pair, transverse momentum of the top quark  $p_T(t)$ , the difference in rapidities between the top quark and the antitop quark  $y(t) - y(\bar{t})$ , the difference in rapidities between the top quark and the boson  $y(t) - y(B)$ , the difference in the azimuthal angle between the top quark and the antitop quark  $\phi(t) - \phi(\bar{t})$ , and the difference in the azimuthal angle between the top quark and the boson  $\phi(t) - \phi(B)$  [34] were computed in the direct QCD approach. Some of these calculations [33–35] involved matching to complete NLO (QCD+EW) result, *i.e.* including all EW and QCD contributions up to NLO in the corresponding coupling constant. Calculations in the framework of the soft-collinear effective theory (SCET) for the  $t\bar{t}H$  process led first to obtaining approximate NNLO [36] and later full NNLL [37] predictions. NNLL+NLO predictions have been obtained in SCET for  $pp \rightarrow t\bar{t}W$  [38, 39] and for  $pp \rightarrow t\bar{t}Z$  in [40]. Results for a set of differential  $t\bar{t}B$  distributions in the SCET approach can be found in [41].

Below we review results for threshold-resummed cross sections  $pp \rightarrow t\bar{t}B$ ,  $B = H, W, Z$  in the invariant mass kinematics, obtained using the Mellin-space approach at NNLL accuracy [32–35], matched to the complete NLO (QCD+EW) predictions.

## 2. Analytical description

In the following, we treat the soft gluon corrections in the invariant mass kinematics, *i.e.* we consider the limit  $\hat{\rho} = Q^2/\hat{s} \rightarrow 1$  with  $Q^2 = (p_t + p_{\bar{t}} + p_B)^2$  and  $\hat{s}$  being the center-of-mass partonic energy. The logarithms resummed in the invariant mass threshold limit have the form of  $\alpha_s^m \left( \frac{\log^n(1-\hat{\rho})}{1-\hat{\rho}} \right)_+$ ,  $m \leq 2n - 1$  with the plus distribution  $\int_0^1 dx(f(x))_+ = \int_0^1 dx(f(x) - f(x_0))$ . The Mellin moments of the differential cross section  $d\sigma_{ij \rightarrow t\bar{t}B}/dQ^2$  are taken with respect to the variable  $\rho = Q^2/S$ , where  $S$  is the hadronic collision energy. At the partonic level, this leads to

$$\begin{aligned} & \frac{d\tilde{\sigma}_{ij \rightarrow t\bar{t}B}}{dQ^2}(N, Q^2, m_t, m_B, \mu_R^2, \mu_F^2) \\ &= \int_0^1 d\hat{\rho} \hat{\rho}^{N-1} \frac{d\hat{\sigma}_{ij \rightarrow t\bar{t}B}}{dQ^2}(\hat{\rho}, Q^2, m_t, m_{W/Z}, \mu_R^2, \mu_F^2) \end{aligned} \quad (1)$$

for the Mellin moments for the process  $ij \rightarrow t\bar{t}B$ , with  $i, j$  denoting two massless colored partons. In the Mellin space, the threshold limit of  $\hat{\rho} \rightarrow 1$  corresponds to the limit  $N \rightarrow \infty$ . Apart from  $N$ , the resummed cross section, Eq. (1), depends also on various characteristic scales for the process: the invariant mass  $Q$ , the masses of the top quark  $m_t$  and of the heavy boson  $m_B$ , and the renormalization and factorization scales,  $\mu_R$  and  $\mu_F$ . Since the process involves more than three colored partons, the resummed cross section is expressed in terms of color matrices. In the Mellin space, the resummed partonic cross section has the form [42, 43] of

$$\frac{d\tilde{\sigma}_{ij \rightarrow t\bar{t}B}}{dQ^2} = \text{Tr} [\mathbf{H}_{ij \rightarrow t\bar{t}B} \mathbf{S}_{ij \rightarrow t\bar{t}B}] \Delta_i \Delta_j, \quad (2)$$

where  $\mathbf{H}_{ij \rightarrow t\bar{t}W/Z}$  and  $\mathbf{S}_{ij \rightarrow t\bar{t}B}$  are color matrices and the trace is taken in color space. We describe the evolution of color in the  $s$ -channel color basis, for which the basis vectors are  $c_1 = \delta_{a_i, a_j} \delta_{a_k, a_l}$ ,  $c_8 = T_{a_i, a_j}^c T_{a_k, a_l}^c$  for the  $q\bar{q}$  initial state and  $c_1 = \delta_{a_i, a_j} \delta_{a_k, a_l}$ ,  $c_{8S} = d_{c, a_i, a_j} T_{a_k, a_l}^c$ ,  $c_{8A} = f_{c, a_i, a_j} T_{a_k, a_l}^c$  for the  $gg$  initial state. This choice of color basis leads to a diagonal soft anomalous dimension matrix in the absolute threshold limit

$(2m_t + m_B)^2/\hat{s} \rightarrow 1$ , which is a special case of the invariant mass threshold limit.  $\mathbf{H}_{ij \rightarrow t\bar{t}B}$  describes the hard scattering contributions projected on the color basis, while  $\mathbf{S}_{ij \rightarrow t\bar{t}B}$  represents the soft wide angle emission. The (soft-) collinear logarithmic contributions from the initial-state partons are taken into account by the functions  $\Delta_i$  and  $\Delta_j$ . They have been known for a long time [44, 45] and depend only on the emitting parton.

The soft function is given by a solution of the renormalization group equation [46, 47]

$$\begin{aligned} \mathbf{S}_{ij \rightarrow klB}(N, Q^2, \mu_F^2, \mu_R^2) &= \bar{\mathbf{U}}_{ij \rightarrow klB}(N, Q^2, \mu_F^2, \mu_R^2) \tilde{\mathbf{S}}_{ij \rightarrow klB}(\alpha_s(Q^2/\bar{N}^2)) \\ &\quad \times \mathbf{U}_{ij \rightarrow klB}(N, Q^2, \mu_F^2, \mu_R^2), \end{aligned} \quad (3)$$

where  $\tilde{\mathbf{S}}_{ij \rightarrow klB}$  plays a role of a boundary condition. This soft matrix, as well as the hard function  $\mathbf{H}_{ij \rightarrow t\bar{t}B}$  can be calculated perturbatively:  $\tilde{\mathbf{S}}_{ij \rightarrow klB} = \tilde{\mathbf{S}}_{ij \rightarrow klB}^{(0)} + \frac{\alpha_s}{\pi} \tilde{\mathbf{S}}_{ij \rightarrow klB}^{(1)} + \dots$ ,  $\mathbf{H}_{ij \rightarrow klB} = \mathbf{H}_{ij \rightarrow klB}^{(0)} + \frac{\alpha_s}{\pi} \mathbf{H}_{ij \rightarrow klB}^{(1)} + \dots$ . At the NNLL accuracy, knowledge of  $\tilde{\mathbf{S}}_{ij \rightarrow klB}^{(1)}$  and  $\mathbf{H}_{ij \rightarrow klB}^{(1)}$  is required, whereas for NLL only leading terms  $\mathbf{H}_{ij \rightarrow klB}^{(0)}, \tilde{\mathbf{S}}_{ij \rightarrow klB}^{(0)}$  are needed.

The soft function evolution matrices  $\mathbf{U}_{ij \rightarrow klB}$  are defined as a path-ordered exponents

$$\mathbf{U}_{ij \rightarrow klB}(N, Q^2, \mu_F^2, \mu_R^2) = \text{P exp} \left[ \int_{\mu_F}^{Q/\bar{N}} \frac{dq}{q} \boldsymbol{\Gamma}_{ij \rightarrow klB}(\alpha_s(q^2)) \right], \quad (4)$$

where the soft anomalous dimension is calculated [30, 48] as a perturbative function in  $\alpha_s$

$$\boldsymbol{\Gamma}_{ij \rightarrow klB}(\alpha_s) = \left( \frac{\alpha_s}{\pi} \right) \boldsymbol{\Gamma}_{ij \rightarrow klB}^{(1)} + \left( \frac{\alpha_s}{\pi} \right)^2 \boldsymbol{\Gamma}_{ij \rightarrow klB}^{(2)} + \dots \quad (5)$$

In order to diagonalize the one-loop soft anomalous dimension matrix, we make use of the transformation [49]

$$\boldsymbol{\Gamma}_R^{(1)} = \mathbf{R}^{-1} \boldsymbol{\Gamma}_{ij \rightarrow klB}^{(1)} \mathbf{R}. \quad (6)$$

Correspondingly, other matrices need to be also transformed using the diagonalization matrix  $\mathbf{R}$ :  $\boldsymbol{\Gamma}_R^{(2)} = \mathbf{R}^{-1} \boldsymbol{\Gamma}_{ij \rightarrow klB}^{(2)} \mathbf{R}$ ,  $\mathbf{H}_R = \mathbf{R}^{-1} \mathbf{H}_{ij \rightarrow klB} (\mathbf{R}^{-1})^\dagger$ ,  $\tilde{\mathbf{S}}_R = \mathbf{R}^\dagger \tilde{\mathbf{S}}_{ij \rightarrow klB} \mathbf{R}$ .

At NLL accuracy, the evolution of the soft matrix  $\mathbf{S}_{ij \rightarrow t\bar{t}B}$  is given by the one-loop anomalous dimension matrix, see *e.g.* [30]. By changing the color basis to  $R$ -basis, the path ordered exponentials in Eq. (4), considered at NLL,

reduce to simple exponentials given in terms of the eigenvalues  $\lambda_I^{(1)}$  of the soft anomalous dimension matrix  $\boldsymbol{\Gamma}_R^{(1)}$ . Together with the LO contributions to the hard and soft function, it results in the following expression for the NLL cross section in the Mellin space:

$$\begin{aligned} \frac{d\tilde{\sigma}_{ij \rightarrow k l B}^{(\text{NLL})}}{dQ^2} (N, Q^2, m_t^2, m_B^2, \mu_F^2, \mu_R^2) &= \boldsymbol{H}_{R,IJ}^{(0)} (Q^2, m_t^2, m_B^2) \tilde{\boldsymbol{S}}_{R,Jl}^{(0)} \\ &\times \Delta^i (N+1, Q^2, \mu_F^2, \mu_R^2) \Delta^j (N+1, Q^2, \mu_F^2, \mu_R^2) \\ &\times \exp \left[ \frac{\log(1-2\lambda)}{2\pi b_0} \left( (\lambda_J^{(1)})^* + \lambda_I^{(1)} \right) \right], \end{aligned} \quad (7)$$

where the color indices  $I$  and  $J$  are implicitly summed over,  $b_0$  is the first coefficient of expansion  $\beta_{\text{QCD}}$  in  $\alpha_s$  and  $\lambda = \alpha_s b_0 \log(N)$ . The trace of the product of two matrices  $\boldsymbol{H}_R^{(0)}$  and  $\tilde{\boldsymbol{S}}_R^{(0)}$  returns the LO cross section. The incoming parton radiative factors  $\Delta_i$  are now considered only at NLL accuracy.

In order to improve the accuracy of the numerical approximation provided by the NLL resummation, it is customary to include terms up to  $\mathcal{O}(\alpha_s)$  in the expansion of the hard and soft function leading to

$$\begin{aligned} \frac{d\tilde{\sigma}_{ij \rightarrow k l B}^{(\text{NLL w C})}}{dQ^2} (N, Q^2, m_t^2, m_B^2, \mu_F^2, \mu_R^2) &= \boldsymbol{H}_{R,IJ} (Q^2, m_t^2, m_B^2, \mu_F^2, \mu_R^2) \\ &\times \tilde{\boldsymbol{S}}_{R,Jl} (Q^2, m_t^2, m_B^2) \Delta^i (N+1, Q^2, \mu_F^2, \mu_R^2) \Delta^j (N+1, Q^2, \mu_F^2, \mu_R^2) \\ &\times \exp \left[ \frac{\log(1-2\lambda)}{2\pi b_0} \left( (\lambda_J^{(1)})^* + \lambda_I^{(1)} \right) \right], \end{aligned}$$

where

$$\boldsymbol{H}_R \tilde{\boldsymbol{S}}_R = \boldsymbol{H}_R^{(0)} \tilde{\boldsymbol{S}}_R^{(0)} + \frac{\alpha_s}{\pi} \left[ \boldsymbol{H}_R^{(1)} \tilde{\boldsymbol{S}}_R^{(0)} + \boldsymbol{H}_R^{(0)} \tilde{\boldsymbol{S}}_R^{(1)} \right].$$

We will refer to this result as “NLL w C”.

We compute the inclusive total cross section by integrating the expression over  $Q^2$ . For the differential distributions of an observable  $\mathcal{O}$ , in addition to the integration over  $Q^2$ , a function  $\mathcal{F}_{\mathcal{O}}$  is introduced. It includes a restriction on the three-particle phase space  $\Phi_3$ , defining the observable  $\mathcal{O}$

$$\begin{aligned} \frac{d\tilde{\sigma}_{ij \rightarrow k l B}^{(\text{NNLL})}}{d\mathcal{O}} (N, \mathcal{O}, m_t^2, m_B^2, \mu_F^2, \mu_R^2) \\ = \int dQ^2 \int d\Phi_3 \text{Tr} [\boldsymbol{H} (Q^2, \Phi_3, m_t^2, m_B^2, \mu_F^2, \mu_R^2) \\ \times \boldsymbol{S} (N+1, Q^2, \Phi_3, m_t^2, m_B^2, \mu_R^2)] \\ \times \Delta^i (N+1, Q^2, \mu_F^2, \mu_R^2) \Delta^j (N+1, Q^2, \mu_F^2, \mu_R^2) \mathcal{F}_{\mathcal{O}} (Q^2, \Phi_3, m_t^2, m_B^2). \end{aligned} \quad (8)$$

The electroweak effects are included additively by matching the resummed QCD calculation to the cross sections calculated at the complete NLO QCD and EW accuracy [50], indicated by NLO (QCD+EW). More specifically, at the LO accuracy, apart from the  $\mathcal{O}(\alpha_s^2\alpha)$  contributions, also the  $\mathcal{O}(\alpha_s\alpha^2)$  and  $\mathcal{O}(\alpha^3)$  terms are included. The complete NLO(QCD+EW) result, besides the  $\mathcal{O}(\alpha_s^3\alpha)$  correction, contains also the  $\mathcal{O}(\alpha_s^2\alpha^2)$ ,  $\mathcal{O}(\alpha_s\alpha^3)$  and  $\mathcal{O}(\alpha^4)$  corrections as well as the above-mentioned LO terms.

### 3. Numerical predictions

The numerical results were obtained using the same set up for input parameters as the one used in the HXSWG Yellow Report 4 [53], *i.e.*  $m_t = 172.5 \text{ GeV}$ ,  $m_H = 125 \text{ GeV}$ ,  $m_W = 80.385 \text{ GeV}$ ,  $m_Z = 91.188 \text{ GeV}$ ,  $G_F = 1.1663787 \times 10^{-5} \text{ GeV}^{-2}$  and the LUXqed17\_plus\_PDF4LHC15\_nnlo\_100 distribution function sets [51, 52, 54–59] with the corresponding values of  $\alpha_s$ . The values of the NLO cross sections are obtained using the MadGraph5\_aMC@NLO code [21, 50], from where we also extract the QCD one loop virtual corrections needed for the hard color matrix  $\mathbf{H}^{(1)}$ . All numerical results for resummed quantities were calculated and cross-checked with two independent in-house Monte Carlo codes.

The predictions for total cross sections at various levels at theoretical accuracy for all three processes of associated top-pair production  $pp \rightarrow t\bar{t}B$ ,  $B = H, Z, W$  are shown in Fig. 1. We calculate the predictions for five choices of the central value of the renormalization and factorization scales:  $\mu_0 = \mu_{F,0} = \mu_{R,0} = Q$ ,  $\mu_0 = \mu_{F,0} = \mu_{R,0} = H_T$ ,  $\mu_0 = \mu_{F,0} = \mu_{R,0} = M/2 = m_t + m_B/2$  and the ‘in-between’ values of  $\mu_0 = \mu_{F,0} = \mu_{R,0} = Q/2$ ,  $\mu_0 = \mu_{F,0} = \mu_{R,0} = H_T/2$ , where  $H_T$  stands for the sum of transverse masses of heavy particles in the final state. The theoretical error due to scale variation is calculated using the so-called 7-point method, where the minimum and maximum values obtained with  $(\mu_F/\mu_0, \mu_R/\mu_0) = (0.5, 0.5), (0.5, 1), (1, 0.5), (1, 1), (1, 2), (2, 1), (2, 2)$  are considered.

Although the NLO(QCD+EW) results for various scale choices span quite a large range of values, we observe the results get closer as the accuracy of resummation improves from NLL to NNLL, indicating the importance of resummed calculations. Another manifestation of the same effect originating from soft gluon corrections is the decrease in the scale uncertainties calculated for each specific scale choice which is also progressing with increasing precision of the theoretical predictions. These trends are much stronger for  $t\bar{t}H$  and  $t\bar{t}Z$  production than for  $t\bar{t}W$  due to the  $gg$  channel contributing to the LO and, correspondingly, to the resummed cross section. Given the conspicuous stability of the NLO(QCD+EW)+NNLL results, we are encouraged to combine our results obtained for various scale choices. For this purpose, we adopt the method proposed by the Higgs Cross Section Working

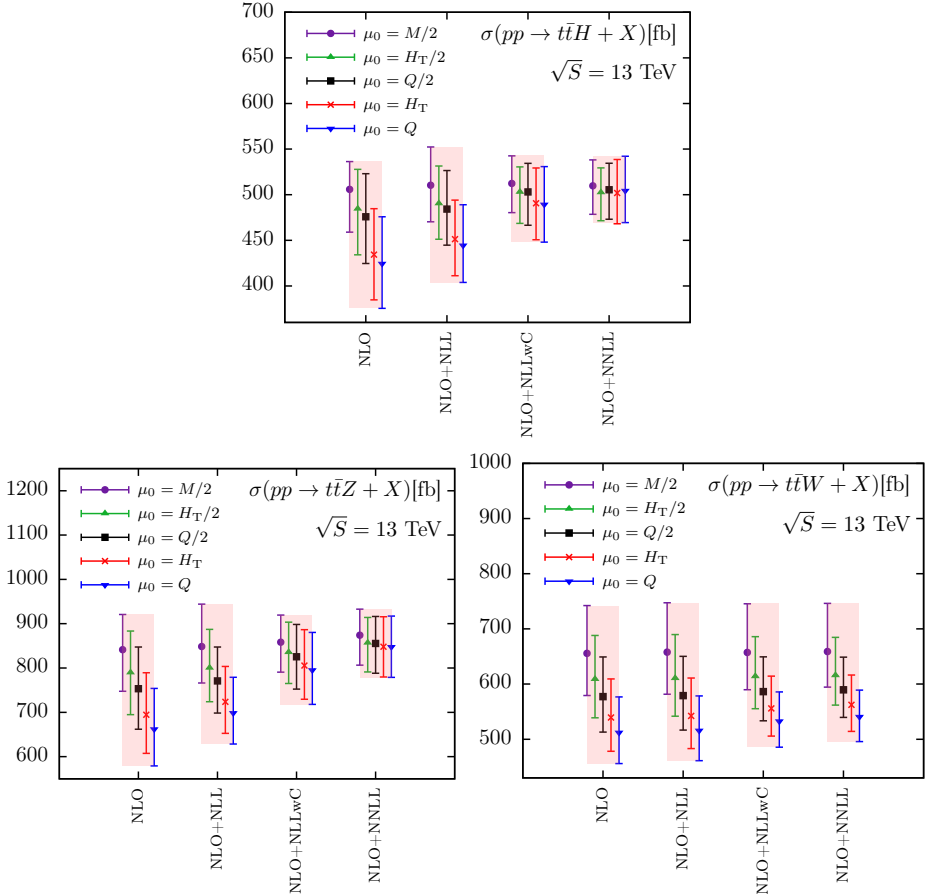


Fig. 1.  $pp \rightarrow t\bar{t}B$  ( $B = H, Z, W$ ) total cross sections at various levels at theoretical accuracy.

Group [60]. In this way, at 13 TeV we obtain

$$\sigma_{ttH}^{\text{NLO+NNLL}} = 504^{+7.6\%+2.4\%}_{-7.1\%-2.4\%} \text{ fb}, \quad (9)$$

$$\sigma_{ttZ}^{\text{NLO+NNLL}} = 859^{+8.6\%+2.3\%}_{-9.5\%-2.3\%} \text{ fb}, \quad (10)$$

$$\sigma_{ttW}^{\text{NLO+NNLL}} = 592^{+26.1\%+2.1\%}_{-16.2\%-2.1\%} \text{ fb}, \quad (11)$$

where the first error is the scale uncertainty, while the second one is the PDF uncertainty of the NLO(QCD+EW) prediction. Comparing the theoretical error for the  $t\bar{t}Z$  cross section listed above with the CMS measurement  $\sigma(t\bar{t}Z) = 0.95 \pm 0.05(\text{stat.}) \pm 0.06(\text{syst.})$  pb [10], it is clear that NNLL resummation brings the accuracy of the theoretical predictions to a level comparable with experimental precision.

As discussed above, the presented formalism allows to study a number of differential distributions. In particular, we have access to observables that are invariant under boosts from the hadronic center-of-mass frame to the partonic center-of-mass frame. In Figs. 2 and 3, we show selected NLO(QCD+EW)+ NNLL distributions for the process with the highest

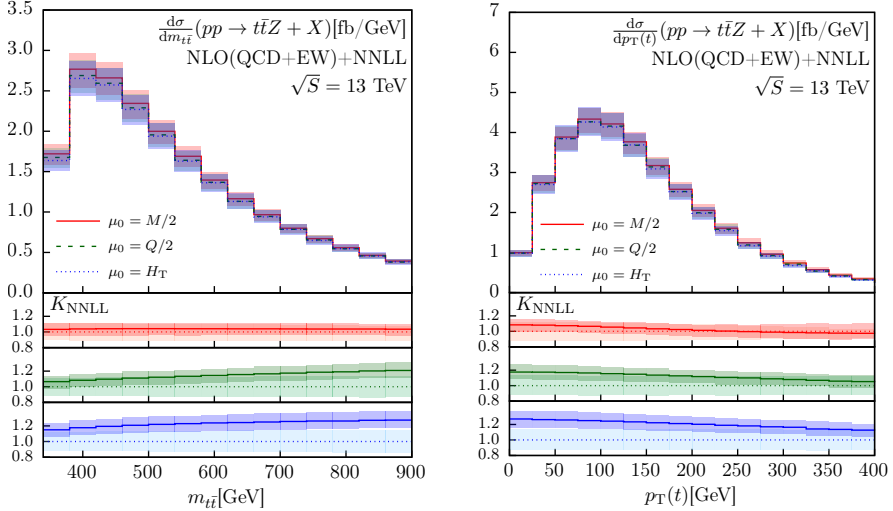


Fig. 2. Predictions for  $pp \rightarrow t\bar{t}Z$  differential cross sections in  $m_{t\bar{t}}$  and  $p_T(t)$ . Lower panels show ratio of the NLO(QCD+EW)+NNLL and NLO(QCD+EW) distributions for three central scale choices  $\mu_0 = M/2$ ,  $\mu_0 = Q/2$  and  $\mu_0 = H_T$ . Only scale uncertainties are shown.

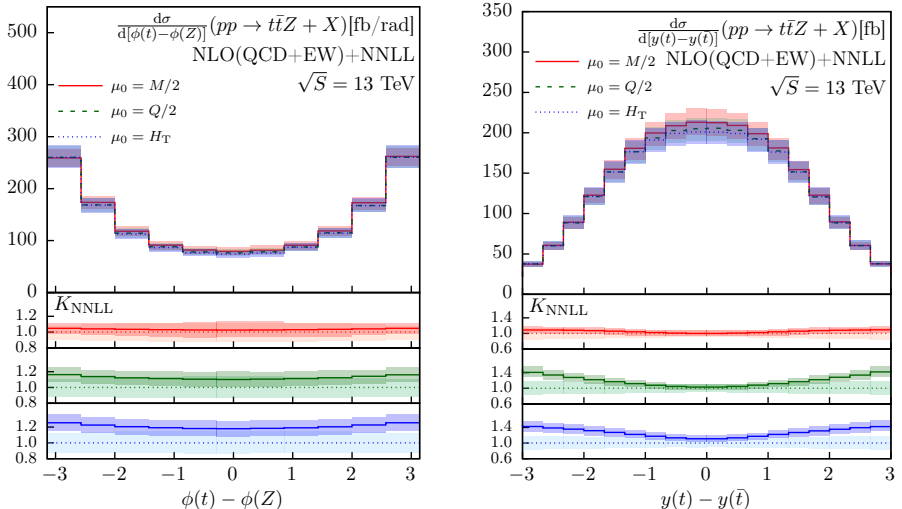


Fig. 3. The same as in Fig. 2 but for differential cross sections in  $\phi(t) - \phi(Z)$  and in  $y(t) - y(\bar{t})$ .

cross section,  $pp \rightarrow t\bar{t}Z$ , for three representative scale choices:  $\mu_0 = M/2$ ,  $\mu_0 = Q/2$  and  $\mu_0 = H_T$ . We refer the reader to [34] for differential cross sections for the  $t\bar{t}H$ ,  $t\bar{t}W$  production as well as additional distributions for the  $t\bar{t}Z$  process. The top panels of Figs. 2, 3 and 4 (left) demonstrate an excellent agreement for the NLO(QCD+EW)+NNLL predictions obtained for the three scale choices. The lower three panels in the figures show ratios of the NLO(QCD+EW)+NNLL distributions to the NLO(QCD+EW) distributions, calculated for different values of  $\mu_0$ . The dark shaded areas indicate the scale errors of the NLO(QCD+EW)+NNLL predictions, while light-shaded areas correspond to the scale errors of the NLO(QCD+EW) results. We observe that the ratios can differ substantially depending on the final state, observable or the central scale. Generally, the NNLL resummation has the biggest impact on the predictions obtained for  $\mu_0 = H_T$  among the three scale choice we study. The ratios show that resummation can contribute as much as *ca.* 30%, up to 40%, correction to the  $t\bar{t}Z$  distribution at this scale choice. Figure 4 focuses on the  $p_T(Z)$  distribution: on the left-hand side, we show the NLO(QCD+EW) + NNLL distributions for the three different scale choices like in Figs. 2 and 3, while the right plot shows a comparison of the CMS data [10] to the NLO(QCD+EW) and our NLO(QCD+EW)+NNLL predictions for the scale choice  $\mu_0 = H_T$ . From the figure, it is clear that the resummed NNLL corrections bring the theoretical predictions closer to data and lead to a significant reduction of the scale dependence error.

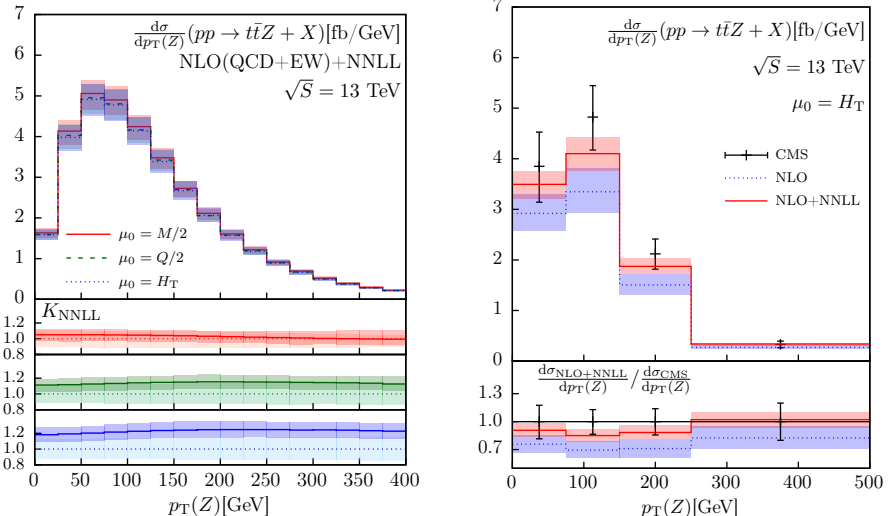


Fig. 4. Transverse momentum distribution  $p_T(Z)$  of the  $Z$  boson produced in the  $pp \rightarrow t\bar{t}Z$  process. Left: The same as in Fig. 2 but for  $p_T(Z)$ . Right: Comparison of the NLO(QCD+EW) and NLO(QCD+EW)+NNLL predictions calculated at  $\mu_0 = H_T$  with the CMS data [10].

This work has been supported by the DFG grant KU3103/2 and the National Science Center, Poland (NCN) grants No. 2017/27/B/ST2/02755 and 2019/32/C/ST2/00202.

## REFERENCES

- [1] CMS Collaboration (A.M. Sirunyan *et al.*), *Phys. Rev. Lett.* **120**, 231801 (2018), [arXiv:1804.02610 \[hep-ex\]](#).
- [2] ATLAS Collaboration (M. Aaboud *et al.*), *Phys. Lett. B* **784**, 173 (2018), [arXiv:1806.00425 \[hep-ex\]](#).
- [3] CMS Collaboration (S. Chatrchyan *et al.*), *Phys. Rev. Lett.* **110**, 172002 (2013), [arXiv:1303.3239 \[hep-ex\]](#).
- [4] CMS Collaboration (V. Khachatryan *et al.*), *Eur. Phys. J. C* **74**, 3060 (2014), [arXiv:1406.7830 \[hep-ex\]](#).
- [5] ATLAS Collaboration (G. Aad *et al.*), *J. High Energy Phys.* **1511**, 172 (2015), [arXiv:1509.05276 \[hep-ex\]](#).
- [6] CMS Collaboration (V. Khachatryan *et al.*), *J. High Energy Phys.* **1601**, 096 (2016), [arXiv:1510.01131 \[hep-ex\]](#).
- [7] ATLAS Collaboration (M. Aaboud *et al.*), *Eur. Phys. J. C* **77**, 40 (2017), [arXiv:1609.01599 \[hep-ex\]](#).
- [8] CMS Collaboration (A.M. Sirunyan *et al.*), *J. High Energy Phys.* **1808**, 011 (2018), [arXiv:1711.02547 \[hep-ex\]](#).
- [9] ATLAS Collaboration (M. Aaboud *et al.*), *Phys. Rev. D* **99**, 072009 (2019), [arXiv:1901.03584 \[hep-ex\]](#).
- [10] CMS Collaboration (A.M. Sirunyan *et al.*), *J. High Energy Phys.* **2003**, 056 (2020), [arXiv:1907.11270 \[hep-ex\]](#).
- [11] W. Beenakker *et al.*, *Phys. Rev. Lett.* **87**, 201805 (2001), [arXiv:hep-ph/0107081](#); *Nucl. Phys. B* **653**, 151 (2003), [arXiv:hep-ph/0211352](#).
- [12] L. Reina, S. Dawson, *Phys. Rev. Lett.* **87**, 201804 (2001), [arXiv:hep-ph/0107101](#); L. Reina, S. Dawson, D. Wackerth, *Phys. Rev. D* **65**, 053017 (2002), [arXiv:hep-ph/0109066](#); S. Dawson, L.H. Orr, L. Reina, D. Wackerth, *Phys. Rev. D* **67**, 071503 (2003), [arXiv:hep-ph/0211438](#); S. Dawson *et al.*, *Phys. Rev. D* **68**, 034022 (2003), [arXiv:hep-ph/0305087](#).
- [13] A. Lazopoulos, T. McElmurry, K. Melnikov, F. Petriello, *Phys. Lett. B* **666**, 62 (2008), [arXiv:0804.2220 \[hep-ph\]](#).
- [14] A. Lazopoulos, K. Melnikov, F.J. Petriello, *Phys. Rev. D* **77**, 034021 (2008), [arXiv:0709.4044 \[hep-ph\]](#).
- [15] V. Hirschi *et al.*, *J. High Energy Phys.* **1105**, 044 (2011), [arXiv:1103.0621 \[hep-ph\]](#).
- [16] R. Frederix *et al.*, *Phys. Lett. B* **701**, 427 (2011), [arXiv:1104.5613 \[hep-ph\]](#).
- [17] M.V. Garzelli, A. Kardos, C.G. Papadopoulos, Z. Trócsányi, *Europhys. Lett.* **96**, 11001 (2011), [arXiv:1108.0387 \[hep-ph\]](#).

- [18] H.B. Hartanto, B. Jager, L. Reina, D. Wackerlo, *Phys. Rev. D* **91**, 094003 (2015), [arXiv:1501.04498 \[hep-ph\]](#).
- [19] A. Kardos, Z. Trócsányi, C. Papadopoulos, *Phys. Rev. D* **85**, 054015 (2012), [arXiv:1111.0610 \[hep-ph\]](#).
- [20] J.M. Campbell, R.K. Ellis, *J. High Energy Phys.* **1207**, 052 (2012), [arXiv:1204.5678 \[hep-ph\]](#).
- [21] J. Alwall *et al.*, *J. High Energy Phys.* **1407**, 079 (2014), [arXiv:1405.0301 \[hep-ph\]](#).
- [22] M.V. Garzelli, A. Kardos, C.G. Papadopoulos, Z. Trócsányi, *Phys. Rev. D* **85**, 074022 (2012), [arXiv:1111.1444 \[hep-ph\]](#).
- [23] M.V. Garzelli, A. Kardos, C.G. Papadopoulos, Z. Trócsányi, *J. High Energy Phys.* **1211**, 056 (2012), [arXiv:1208.2665 \[hep-ph\]](#).
- [24] S. Frixione *et al.*, *J. High Energy Phys.* **1409**, 065 (2014), [arXiv:1407.0823 \[hep-ph\]](#).
- [25] S. Frixione *et al.*, *J. High Energy Phys.* **1506**, 184 (2015), [arXiv:1504.03446 \[hep-ph\]](#).
- [26] Y. Zhang *et al.*, *Phys. Lett. B* **738**, 1 (2014), [arXiv:1407.1110 \[hep-ph\]](#).
- [27] A. Denner, R. Feger, *J. High Energy Phys.* **1511**, 209 (2015), [arXiv:1506.07448 \[hep-ph\]](#).
- [28] G. Bevilacqua *et al.*, *J. High Energy Phys.* **1911**, 001 (2019), [arXiv:1907.09359 \[hep-ph\]](#).
- [29] A. Denner, J.N. Lang, M. Pellen, S. Uccirati, *J. High Energy Phys.* **1702**, 053 (2017), [arXiv:1612.07138 \[hep-ph\]](#).
- [30] A. Kulesza, L. Motyka, T. Stebel, V. Theeuwes, *J. High Energy Phys.* **1603**, 065 (2016), [arXiv:1509.02780 \[hep-ph\]](#).
- [31] A. Kulesza, L. Motyka, T. Stebel, V. Theeuwes, *PoS LHCP2016*, 084 (2016), [arXiv:1609.01619 \[hep-ph\]](#).
- [32] A. Kulesza, L. Motyka, T. Stebel, V. Theeuwes, *Phys. Rev. D* **97**, 114007 (2018), [arXiv:1704.03363 \[hep-ph\]](#).
- [33] A. Kulesza *et al.*, *Eur. Phys. J. C* **79**, 249 (2019), [arXiv:1812.08622 \[hep-ph\]](#).
- [34] A. Kulesza *et al.*, [arXiv:2001.03031 \[hep-ph\]](#).
- [35] A. Kulesza *et al.*, [arXiv:1905.07815 \[hep-ph\]](#).
- [36] A. Broggio *et al.*, *J. High Energy Phys.* **1603**, 124 (2016), [arXiv:1510.01914 \[hep-ph\]](#).
- [37] A. Broggio, A. Ferroglio, B.D. Pecjak, L.L. Yang, *J. High Energy Phys.* **1702**, 126 (2017), [arXiv:1611.00049 \[hep-ph\]](#).
- [38] H.T. Li, C.S. Li, S.A. Li, *Phys. Rev. D* **90**, 094009 (2014), [arXiv:1409.1460 \[hep-ph\]](#).
- [39] A. Broggio, A. Ferroglio, G. Ossola, B.D. Pecjak, *J. High Energy Phys.* **1609**, 089 (2016), [arXiv:1607.05303 \[hep-ph\]](#).
- [40] A. Broggio *et al.*, *J. High Energy Phys.* **1704**, 105 (2017), [arXiv:1702.00800 \[hep-ph\]](#).

- [41] A. Broggio *et al.*, *J. High Energy Phys.* **1908**, 039 (2019), [arXiv:1907.04343 \[hep-ph\]](#).
- [42] H. Contopanagos, E. Laenen, G.F. Sterman, *Nucl. Phys. B* **484**, 303 (1997), [arXiv:hep-ph/9604313](#).
- [43] N. Kidonakis, G. Oderda, G.F. Sterman, *Nucl. Phys. B* **531**, 365 (1998), [arXiv:hep-ph/9803241](#).
- [44] S. Catani, M.L. Mangano, P. Nason, L. Trentadue, *Nucl. Phys. B* **478**, 273 (1996), [arXiv:hep-ph/9604351](#).
- [45] R. Bonciani, S. Catani, M.L. Mangano, P. Nason, *Nucl. Phys. B* **529**, 424 (1998), [arXiv:hep-ph/9801375](#).
- [46] N. Kidonakis, G. Sterman, *Nucl. Phys. B* **505**, 321 (1997), [arXiv:hep-ph/9705234](#).
- [47] M. Czakon, A. Mitov, G.F. Sterman, *Phys. Rev. D* **80**, 074017 (2009), [arXiv:0907.1790 \[hep-ph\]](#).
- [48] A. Ferroglia, M. Neubert, B.D. Pecjak, L.L. Yang, *Phys. Rev. Lett.* **103**, 201601 (2009), [arXiv:0907.4791 \[hep-ph\]](#).
- [49] N. Kidonakis, G. Oderda, G. Sterman, *Nucl. Phys. B* **525**, 299 (1998), [arXiv:hep-ph/9801268](#).
- [50] R. Frederix *et al.*, *J. High Energy Phys.* **1807**, 185 (2018), [arXiv:1804.10017 \[hep-ph\]](#).
- [51] A. Manohar, P. Nason, G.P. Salam, G. Zanderighi, *Phys. Rev. Lett.* **117**, 242002 (2016), [arXiv:1607.04266 \[hep-ph\]](#).
- [52] A.V. Manohar, P. Nason, G.P. Salam, G. Zanderighi, *J. High Energy Phys.* **1712**, 046 (2017), [arXiv:1708.01256 \[hep-ph\]](#).
- [53] LHC Higgs Cross Section Working Group (D. de Florian *et al.*), [arXiv:1610.07922 \[hep-ph\]](#).
- [54] J. Butterworth *et al.*, *J. Phys. G: Nucl. Part. Phys.* **43**, 023001 (2016), [arXiv:1510.03865 \[hep-ph\]](#).
- [55] S. Dulat *et al.*, *Phys. Rev. D* **93**, 033006 (2016), [arXiv:1506.07443 \[hep-ph\]](#).
- [56] L.A. Harland-Lang, A.D. Martin, P. Motylinski, R.S. Thorne, *Eur. Phys. J. C* **75**, 204 (2015), [arXiv:1412.3989 \[hep-ph\]](#).
- [57] NNPDF Collaboration (R.D. Ball *et al.*), *J. High Energy Phys.* **1504**, 040 (2015), [arXiv:1410.8849 \[hep-ph\]](#).
- [58] J. Gao, P. Nadolsky, *J. High Energy Phys.* **1407**, 035 (2014), [arXiv:1401.0013 \[hep-ph\]](#).
- [59] S. Carrazza *et al.*, *Eur. Phys. J. C* **75**, 369 (2015), [arXiv:1505.06736 \[hep-ph\]](#).
- [60] LHC Higgs Cross Section Working Group Collaboration (S. Dittmaier *et al.*), [arXiv:1101.0593 \[hep-ph\]](#).